

CHAPTER 176

METHOD OF ESTIMATING THE POWER EXTRACTED BY FIXED COASTAL TYPE WAVE POWER EXTRACTORS

Kenji YANO,¹ Hideo KONDO,² M.ASCE and Tomiji WATABE³

ABSTRACT

Study is performed on a vertical flap type energy converter, "Pendulor System". The power absorbed with the system in random waves is estimated using a transfer function of absorbed power (absorption coefficient) in regular waves and wave spectrum. A boundary element technique is applied to compute the hydrodynamic problem associated with the system which is placed in regular waves. The applicability of the method has been examined by a series of field test at a test plant caisson. The agreement between estimation and experiment was found to be good except near the resonance frequency of the system.

1. INTRODUCTION

A large variety of apparatus have been proposed for absorbing wave power and converting to other usable power. These absorbers may be classified roughly into two types, namely, floating type and fixed ones. Initially the fixed type ones had been discarded since the incident wave energy at shallow water area becomes less than that at the deep water. So, they unlikely seem to be attractive. However, since the floating type absorbers accompanies with difficult problems such as mooring or positioning system, energy transportation to land and maintenance which raise the cost of energy. This leads us to a bottom standing fixed type device at the coastal area which can serve as a breakwater and may save the energy cost.

With this point of view, we have studied the fixed type absorbers which can be set within coastal structures and had developed a few systems such as the "Pendulor System", a kind of pendulum with a flat plate. The system has an excellent power absorbing capacity, which had been introduced at the 19th Conference (Kondo et al, 1984). The present report deals with the method to estimate quantitatively the power absorbed by the pendulor system which will be set linearly alongshore in coastal area. This is one of the major problems to be solved in advance of realizing the commercial systems of fixed type.

1 Research Associate of Civil Engineering, Muroran Institute of Technology, 27-1 Mizumoto-cho, Muroran-Shi, Hokkaido, 050 JAPAN

2 Professor of Civil Engineering, ditto

3 Professor of Mechanical Engineering, ditto

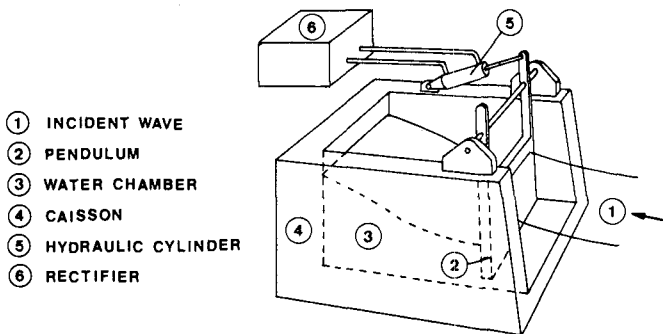


Fig. 1 Schematic diagram of pendulum system

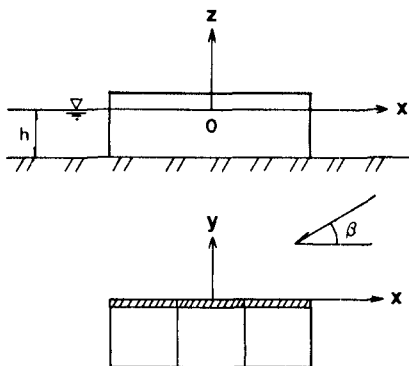


Fig. 2 Co-ordinate system

2. PENDULOR CONCEPT

Fig. 1 shows a concept of the pendulor system. The device consists of an oscillating pendulum around a horizontal axis, a double acting hydraulic cylinder connected to the pendulum, hydraulic circuit, that is a power takeoff mechanism, and a caisson in which a closed water chamber is formed. A kind of standing wave is produced in the chamber by the oscillating pendulum. At the node of standing wave, the pendulum is less affected reacting moment by the wave. Thus the device has high absorption capability under this hydrodynamic condition.

3. THEORETICAL MODEL

3.1 Absorbed Power in Regular and Random Waves

Let's consider m identical pendulor devices connected together to form a string as shown in Fig. 2. Each pendulum is allowed to move roll mode alone in response to regular wave with amplitude a . It is assumed that the mechanism for wave power absorption can be described

by a simple external damper connected to pendulum and that the damping moment caused by power absorption is linearly related to the velocity of the motion of the pendulum.

The motion of pendulums in waves, with their amplitudes varying sinusoidally in time, are calculated by the following equations

$$I_k \ddot{\theta}_k + N_k \dot{\theta}_k + K_k \theta_k = M_k \quad k=1, 2, \dots, m \quad (1)$$

where I_k , K_k and N_k are the moment of inertia, the restoring moment coefficient of the k th pendulum and the damping moment coefficient of the damper attached to the k th pendulum and θ_k is the angular displacement with complex amplitude $\bar{\theta}_k$. M_k is the hydrodynamic moment acting on the k th pendulum and is represented, as follows

$$M_k = M_{0k} - \sum_{\ell=1}^m (I_k \ell \ddot{\theta}_\ell + N_k \ell \dot{\theta}_\ell) \quad (2)$$

where M_{0k} is wave exciting moment associated with incident and scattering waves and the terms in the parentheses are moments on the k th pendulum due to a radiation wave produced by a motion of the ℓ th pendulum. The coefficients I_k and N_k are known as the added moment of inertia and the damping moment coefficient, respectively. The simultaneous linear equations of 1 can be solved for the pendulum motions $\bar{\theta}_k$. Hence, the transfer function of the k th pendulum is defined by Eq. 3.

$$Z_k(f, \beta) = \bar{\theta}_k / a \quad (3)$$

The total power absorbed P_a is given by

$$P_a = \sum_k \frac{1}{2} \omega^2 N_k |\bar{\theta}_k|^2, \quad \omega = 2\pi f \quad (4)$$

The absorbing coefficient κ is defined as

$$\kappa = P_a / (P_w \cdot B_0) \quad (5)$$

where P_w is mean power per unit crest length of incident wave train and B_0 is total width of the series of devices.

It is important for the design of wave power absorbers to know how effectively they absorb power from random waves. In random waves absorbed power \bar{P}_a with the system can be estimated by

$$\bar{P}_a = \rho g \int_0^\infty \int_0^{2\pi} \kappa(f, \beta) S(f, \beta) C_g df d\beta \quad (6)$$

where $\kappa(f, \beta)$ the absorbing coefficient in waves at frequency f in direction β , and $S(f, \beta)$ the directional wave spectrum, ρ the density of the fluid, g the acceleration of gravity and c_g is the group velocity of waves.

For a case that the wave dimensions are known only at deep water, the following relationship is useful for the transformation of a deep water directional spectrum into a shallow water directional spectrum.

$$S(f, \beta) df d\beta C_g = S_0(f, \beta_0) df d\beta_0 K_r^2 \quad (7)$$

where K_r the refraction coefficient and subscript 0 is used for the symbols at deep water. Substituting Eq. 7 into Eq. 6, the absorbed

power at shallow water area is estimated by deep water spectrum using Eq. 8.

$$\begin{aligned} \bar{P}_a &= \rho g \int_0^\infty \int_0^{2\pi} K_R^2(f, h, \beta_0) S_0(f, \beta_0) \\ &\quad \times \kappa(f, \lambda(f, \beta_0)) C_{g0} df d\beta_0 \end{aligned} \tag{8}$$

$$\beta = \lambda(f, \beta_0)$$

where $\lambda(f, \beta_0)$ is a function of the wave direction.

If we used a spreading function D , the directional spectrum is rewritten as follows

$$S_0(f, \beta_0) = S_0(f) D(f, \beta_0, \bar{\beta}_0) \tag{9}$$

where $\bar{\beta}_0$ is the dominant wave direction, $S_0(f)$ is a usual frequency spectrum.

The absorbed power with the system is calculated by finite set of directional and frequency-wise components of the absorption coefficient, the wave spectrum, and so on.

3.2 Hydrodynamic Loads

The hydrodynamic loads acting on the pendulums are computed from the velocity potential along the body boundaries. To obtain the potential, we consider separately the fluid region exterior of the string (outer region) and the region interior of the closed chambers (inner region, excluded "harbor" which is shown below).

In the usual manner the velocity potential in the outer region can be decomposed into

$$\Phi(x, y, z; t) = (\phi_0 + \phi_d + \sum_{k=1}^m \bar{\theta}_k \phi_k) e^{-i\omega t} \tag{10}$$

where ϕ_0 is the known potential of the incident wave and ϕ_d is the diffraction potential corresponding to scattering of the incident waves by the string with fixed pendulums. ϕ_k represents the radiation potential induced by the forced motion of the k th pendulum in the absence of the incident waves. The boundary condition at the body surface are given by

$$\frac{\partial \phi_d}{\partial n} = - \frac{\partial \phi_0}{\partial n} \quad \text{on } \Gamma \tag{11}$$

$$\begin{aligned} \frac{\partial \phi_k}{\partial n} &= -i\omega(z_0 - z) n_y \quad \text{on } \Gamma_k \\ &= 0 \quad \text{on } \Gamma - \Gamma_k \end{aligned} \tag{12}$$

where z_0 represents a depth of the point of rolling axis of the pendulum, Γ_k a wetted surface of the k th pendulum, Γ a wetted surface of the body, n the distance in the direction of the unit normal vector \mathbf{n} directed outward from the boundary and n_y the y -component of \mathbf{n} . In the chamber, the potential ϕ' associated with the unit motion of the pendulum can be treated as two dimensional wave making problem and the solution was obtained by Asano (1980).

Assuming the each chamber has same dimensions, the hydrodynamic

loads and the coefficients are expressed as follows

$$M_{0k} = i\omega\rho e^{-i\omega t} \int_{\Gamma_k} (\phi_0 + \phi_d) \bar{h} d\Gamma \quad (13)$$

$$I_{k\ell} = \frac{1}{\omega^2} \operatorname{Re} [i\omega\rho \int_{\Gamma_k} (\phi_\ell + \delta_{k\ell} \phi') \bar{h} d\Gamma] \quad (14)$$

$$N_{k\ell} = \frac{1}{\omega} \operatorname{Im} [i\omega\rho \int_{\Gamma_k} (\phi_\ell + \delta_{k\ell} \phi') \bar{h} d\Gamma] \quad (15)$$

in which $\delta_{k\ell}$ is the Kronecker delta function, $\bar{h} = (z_0 - z)n_y$, $\operatorname{Re}[\]$ and $\operatorname{Im}[\]$ indicate the real and imaginary parts, respectively.

3.3 Numerical Determination of Potentials

The most general method for calculating the potentials is a boundary element method. A Green's function, G , is chosen as a source potential of unit strength which satisfies the same boundary conditions as the wave potential. As a result of Green's Theorem, the solution for wave potential can be represented as follows

$$-\frac{1}{2} \phi_k(P) = \int_{\Gamma} [\phi_k(Q) \frac{\partial}{\partial n} G(P, Q) - G(P, Q) \frac{\partial}{\partial n} \phi_k(Q)] \quad (16)$$

in which P and Q represent points on the boundary of the body Γ . The corresponding integral equation for ϕ_d is obtained from Eq. 16 by replacing ϕ_k by ϕ_d .

Let ψ represents the unknown potential above mentioned and $\hat{\psi}$ is its derivative. Equation 16 is numerically solved for a ψ at a number of discrete points. The surface Γ of the body is divided into N boundary elements. The values of ψ and $\hat{\psi}$ are assumed to be constant on each element and equal to the values at the element center called "nodes". Hence, the integral Eq. 16 for a particular node 'i' can be approximated as

$$\sum_j \hat{H}_{ij} \psi_j = \sum H_{ij} \hat{\psi}_j \quad (17)$$

$$\hat{H}_{ij} = \frac{1}{2} \delta_{ij} + \int_{\Gamma_j} \frac{\partial}{\partial n} G(i, j) d\Gamma \quad (18)$$

$$H_{ij} = \int_{\Gamma_j} G(i, j) d\Gamma$$

where Γ_j is the boundary of element 'j'. The whole set of equations for N nodes can be expressed in matrix form as follows,

$$\hat{H}U = HQ \quad (19)$$

where

$$\begin{aligned} \hat{H} &= [\hat{H}_{ij}] & \mathbf{H} &= [H_{ij}] \\ \mathbf{U} &= \{\psi_1, \psi_2, \dots, \psi_N\}^T & \mathbf{Q} &= \{\hat{\psi}_1, \hat{\psi}_2, \dots, \hat{\psi}_N\}^T \end{aligned} \quad (20)$$

If a single pendulor system has a "harbor" (Ambli et al,1982), consisting of two parallel projecting sidewalls as shown in Fig. 3, corresponding potentials are obtained by a method of combination of regions (e.g. Brebbia, 1980). Consider two separate solution regions, the open sea (region 1) and inside the harbor (region 2). For the first region, the Eq. 16 can be partitioned as follow,

$$[\hat{H}_0^1 \hat{H}_I^1] \begin{Bmatrix} U_0^1 \\ U_I^1 \end{Bmatrix} = [H_0^1 H_I^1] \begin{Bmatrix} Q_0^1 \\ Q_I^1 \end{Bmatrix} \tag{21}$$

where superscript 1 indicates that it belongs to region 1, subscript I and 0 indicate the mouth of harbor and other boundary of the region 1, respectively. For the second region we have

$$[H_0^2 H_I^2 H_P^2] \begin{Bmatrix} U_0^2 \\ U_I^2 \\ U_P^2 \end{Bmatrix} = [H_0^2 H_I^2 H_P^2] \begin{Bmatrix} Q_0^2 \\ Q_I^2 \\ Q_P^2 \end{Bmatrix} \tag{22}$$

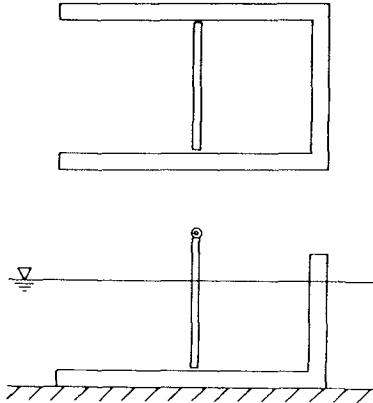


Fig. 3 Geometry of a system added "harbor"

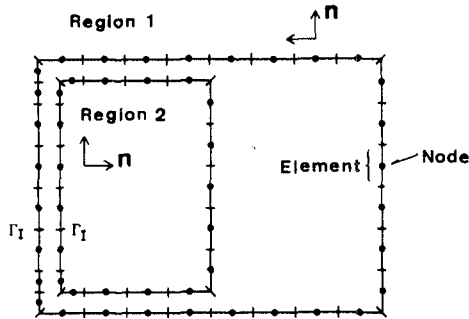


Fig. 4 Body divided into two regions

where subscript P indicate the pendulum part of region 2. According to the definition of the direction of the unit normal vector shown in Fig. 4, the conditions of the mouth of harbor are given by

$$\left. \begin{aligned} \underline{U}_I^1 &= \underline{U}_I^2 \\ \underline{Q}_I^1 &= -\underline{Q}_I^2 \end{aligned} \right\} \quad (\text{radiation problem}) \quad (23)$$

$$\left. \begin{aligned} \underline{U}_I^1 + \underline{u}_I &= \underline{U}_I^2 \\ \underline{Q}_I^1 + \underline{q}_I &= -\underline{Q}_I^2 \end{aligned} \right\} \quad (\text{diffraction problem}) \quad (24)$$

where

$$\underline{U} = \{\phi_{0,1}, \phi_{0,2}, \dots, \phi_{0,N}\} \quad \underline{Q} = \{\hat{\phi}_{0,1}, \hat{\phi}_{0,2}, \dots, \hat{\phi}_{0,N}\} \quad (25)$$

Using Eq. 11, 12 and these conditions, Eq. 21 and Eq. 22 can be rewritten as follows.

$$\begin{bmatrix} \hat{H}_0^1 & \hat{H}_I^1 - H_I^1 & 0 & 0 \\ 0 & \hat{H}_I^2 & H_I^2 & \hat{H}_0^2 \hat{H}_P^2 \end{bmatrix} \begin{Bmatrix} \underline{U}_0^1 \\ \underline{U}_I^1 \\ \underline{Q}_I^1 \\ \underline{U}_0^2 \\ \underline{U}_I^2 \end{Bmatrix} = \begin{bmatrix} 0 \\ H_P^2 \end{bmatrix} \{ \underline{Q}_P^2 \} \quad (26)$$

(radiation problem)

$$= - \begin{bmatrix} 0 & 0 \\ \hat{H}_I^2 & H_I^2 \end{bmatrix} \begin{Bmatrix} \underline{u}_I \\ \underline{q}_I \end{Bmatrix} - \begin{bmatrix} H_0^1 \\ 0 \end{bmatrix} \{ \underline{Q}_0 \} \quad (27)$$

(diffraction problem)

4. FIELD TEST

4.1 Experimental Set-Up

The test plant caisson employed in the field experiment had been constructed seaward of the south breakwater of Port Muroran, as shown in Fig. 5 and Fig. 6. Since the port faces to a bay on the Pacific south west coast of Hokkaido Island, the waves of which significant wave height is greater than 1.0 meter is approximately 12 % and appear mostly in winter.

Fig. 7 shows the dimensions of the caisson. The caisson is partitioned into two chambers by sidewall, and the pendulum had been installed at 2.5 meter inside from the front face of the right hand chamber. The pendulum is of 2.5 ton in weight. Distance between the center of the rolling axis and lower edge of the pendulum is 7.2 meter. The plate to receive wave force at the lower part of it is 2 meter wide and 3.5 meter high.

The wave-induced motion of pendulum is converted into hydraulic

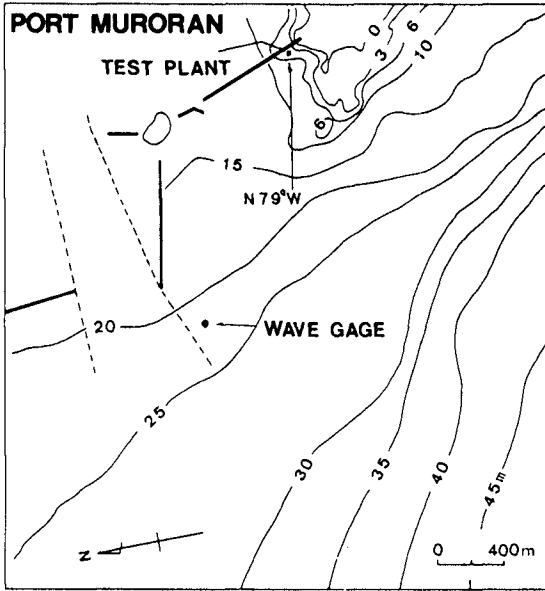


Fig. 5 Location map

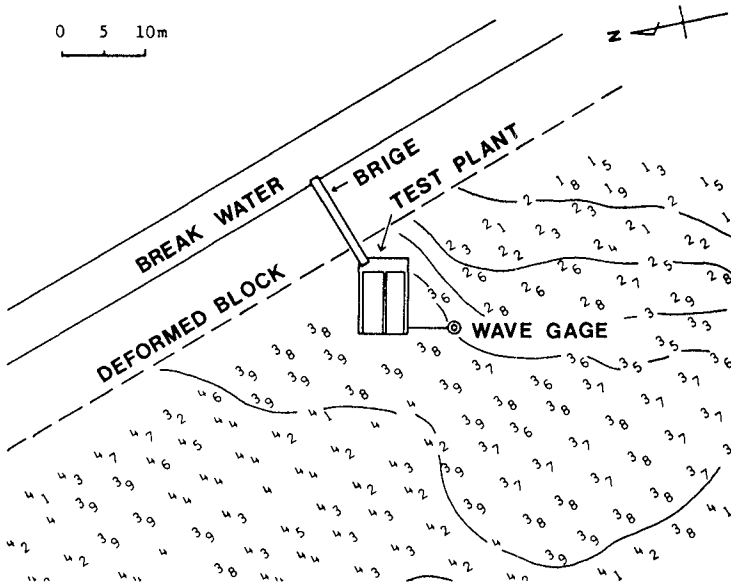


Fig. 6 Bathymetry around test plant

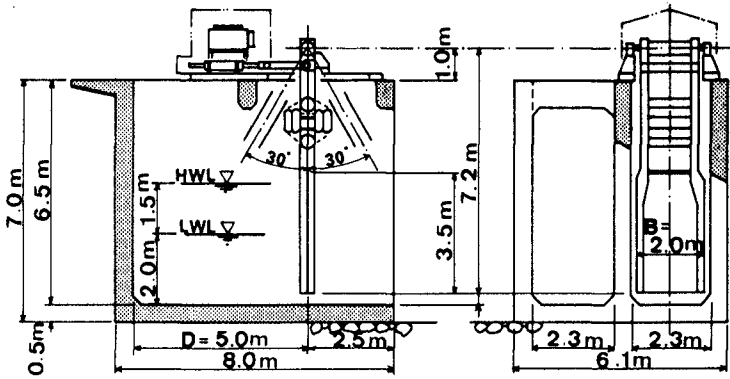


Fig. 7 Dimensions of test plant

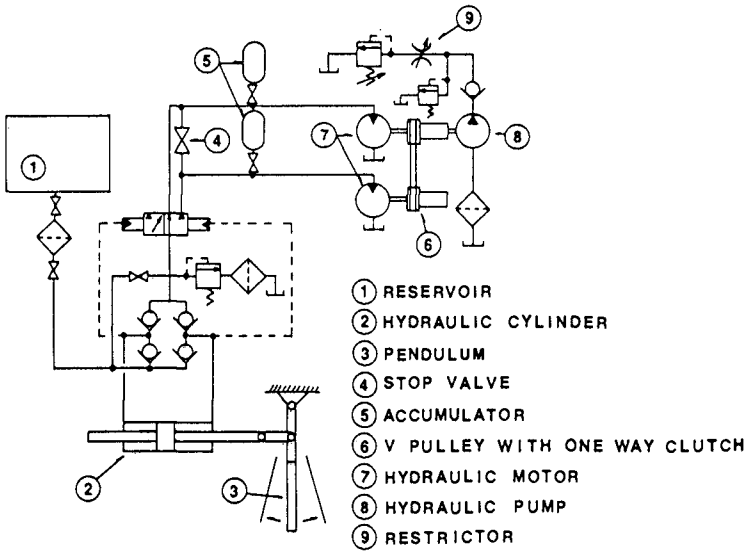


Fig. 8 Hydraulic circuit of test plant

power by the hydro-static power transmission circuit shown in Fig. 8. An electric generator was not equipped in the circuit. The energy absorption is achieved by combination of the hydraulic pump 8 and the restrictor 9, and the energy is finally absorbed by heating oil. In this circuit, the reaction moment of the energy absorption mechanism is non-linear due to the effects of the accumulators 5. Details of the power extracting facilities had been shown by Watabe, et al, in 1986.

The measured quantities in the field tests are the incoming wave profile, displacement of the piston rod, the cylinder pressures P1, P2, total torque of the motors, and the speed of motors. The wave data were measured 5 meter apart from the caisson with the ultrasonic wave gage above sea surface. In addition, the dominant wave direction is measured visually with a compass. In some experiments, the wave data were collected at the location of 1.8 km offshore from the test plant. The data signals were recorded on a magnetic-tape recorder. The measured records were digitized with the sampling rate 2 Hz for a period 1200 seconds giving 2400 data points per measured channel.

4.2 Test Results

(1) Pendulum Motion with/without Damper

Fig. 9 shows the comparison of theoretical and experimental spectra of pendulum motion under the condition of no-load. The former were calculated from the transfer function using measured wave spectrum and a cosine-power spreading function. The influence of the sidewalls protruding in front of the pendulum is considered in the calculation. In the figure, $S_{\theta\theta}$ denotes the power spectrum of the angular displacement of the pendulum and the broken line shows the numerical result for the present pendulum system.

Fig. 10 gives the example of the spectra of wave and pendulum motion with power absorption. In this case, it is necessary a suitable linear approximation of reaction moment of damper to calculate the motion from the mathematical model.

Let's assume that the load system of damper can be defined as follows,

$$M = (i\omega N + K)\bar{\theta} e^{i\omega t} \quad (28)$$

where N and K are an equivalent linearized load damping coefficient and restoring moment coefficient, respectively. So, they are given by

$$N = \frac{1}{\omega} \text{Im} [S_{\theta M} / S_{\theta\theta}]$$

$$K = \text{Re} [S_{\theta M} / S_{\theta\theta}] \quad (29)$$

where $S_{\theta M}$ is the cross-spectrum of angular displacement of pendulum and the reaction moment from the cylinder. Of course, the coefficients N and K are functions of frequency. For simplicity, we used the values of N and K at peak frequency of the spectrum of reacting moment for calculation at arbitrary frequency.

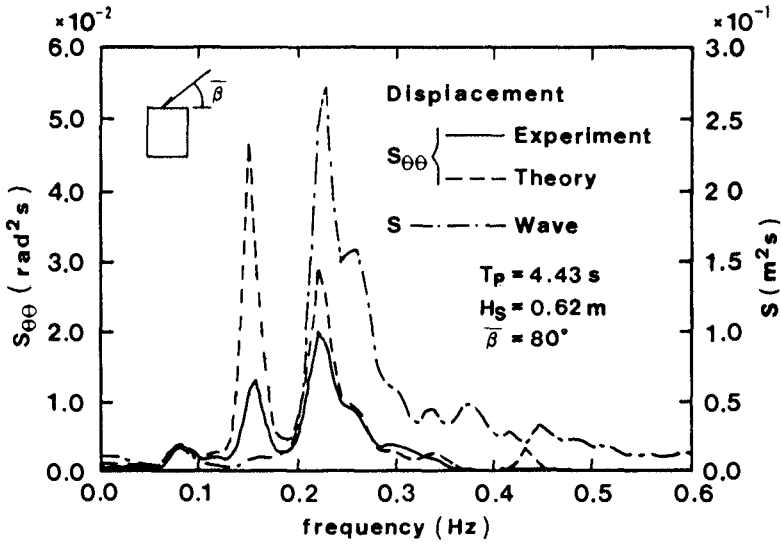


Fig. 9 Spectra of wave and pendulum motion (no-load condition)

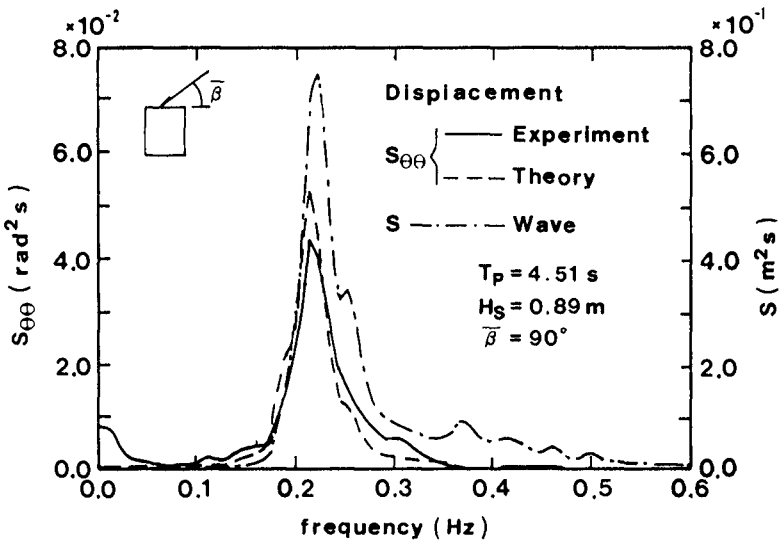


Fig. 10 Spectra of wave and pendulum motion (with power absorption)

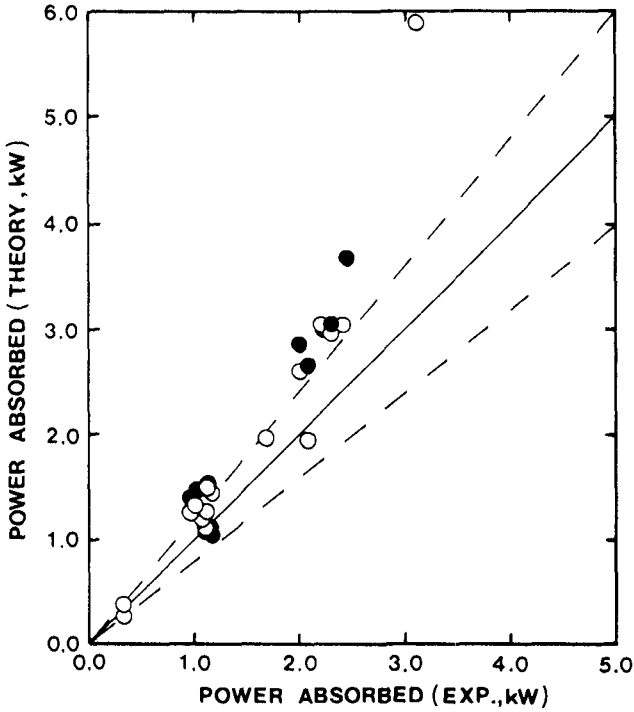


Fig. 11 Comparison of theory with experiment of absorbed power

(2) Absorption Characteristics

Using the estimated spectrum of pendulum motion and the linearized load damping coefficient, we can obtain absorbed power theoretically.

Fig. 11 represents the result of comparison of the theoretical power absorbed with experimental ones at the cylinder. The latter is obtained numerically as follows,

$$\bar{P}_a = \frac{1}{T_m} \int_0^{T_m} A_s (P_1 - P_2) V dt \tag{30}$$

where T_m denotes the recording time of data signals, P_1, P_2 are cylinder pressures, A_s the cross sectional area of piston and V is the velocity of piston.

In the figure, the symbol of solid circle indicates the value estimated from the deep water spectrum. The broken lines represent the range within 20 percent error.

The dominant wave direction of deep water is estimated from wind

direction collected at a small island located nearby the wave gage. The refraction coefficients and wave angles at the plant associated with the deep water waves were determined from wave refraction diagrams.

As concerns the one extreme overestimation plot in the figure, the experimental data was obtained on condition that significant wave height is 1.16 meter and peak frequency of the wave spectrum is near the resonance frequency predicted in the theory.

5. CONCLUDING REMARKS

We have shown a numerical approach to estimate quantitatively the power absorbed by pendulum system of coastal type and confirmed its applicability by the field tests. As expected, one of the main cause of the overestimation above mentioned probably lies that the theory ignores the viscous loss with water motion near the pendulum and that at the mouth of the protruding sidewalls. Another probable cause is due to the partial reflection from the inside surface of the protruding sidewalls, especially the surface of pendulum.

The data obtained from field tests are not enough to allow a more detailed discussion. It is necessary subsequently to assess behavior of the system including the sources of the reduction of absorption in a full range of wave conditions. Stability of the caisson as well as durability of moving components of the system against wave force has been studied and will be disclosed in the near future.

REFERENCES

- 1) Ambli, N., K. Bonke, O. Malmo and A. Reitan (1982). The Kvaener multiresonant OWC, Proc. of 2nd Int. Symp. on Wave Energy Utilization, Trondheim, pp. 275-295.
- 2) Asano, S. (1980). Energy absorption efficiency of flap type wave energy converter, JTTC, SK60-14, (in Japanese).
- 3) Brebbia, C. A. and S. Walked (1980). Boundary element techniques in engineering, Newnes-Butterworths, London, 210p.
- 4) Kondo, H., T. Watabe and K. Yano (1984). Wave power extraction at coastal structure by means of moving body in the chamber, Proc. 19th Coastal Eng. Conf., Houston, III, pp. 2375-2891.
- 5) Watabe, T., H. Kondo and K. Yano (1986). Studies on a pendulum-type wave energy converter, Proc. of 3rd Int. Symp. on Wave, Tidal, OTEC, and Small Scale Hydro Energy, Brighton, pp. 281-292.